Electromagnetic Analysis on Dual-Stator Switched Reluctance Motor

(Mon-Af-Po1.04)

Hao Chen[1], Rui Nie[1], Tong Xu[1]

1. China University of Mining and Technology, Xuzhou 221116, China.

CUMT

Introduction

A novel structure switched reluctance motor with dual stators is presented in this paper which consists of an outer stator, an inner stator, a rotor and two airgaps. In order to maximum the electromagnetic torque of the proposed machine, sensitivity analysis on some geometric dimensions is conducted. These dimensions include pole-arc coefficient, and yoke thickness of stators and rotor. The final geometric dimensions are given in the paper. According to the positive and negative distribution of stator poles and different layouts, windings of this machine have 12 kinds of layouts which are studied in section IV. Based on the finite element calculation result, the average torque of rotor with NSNSNSNSNSNS polarity distribution of outer-stator and SNSNSN polarity distribution of inner-stator is the largest so that this connection pattern of winding is selected. Some transient simulation results are given in this paper which prove the good performance of the dual-stator switched reluctance motor.

Structure of DS-SRM

The structure of the novel machine DS-SRM is shown 1n Fig. 1. The outer-stator adopts salient pole structure of 12 poles, the inner-stator adopts 6 poles, and the middle-rotor is doubly salient with 8 poles. The outer motor is three-phase 12/8 structure machine, and the inner motor is three-phase 6/8 structure machine.

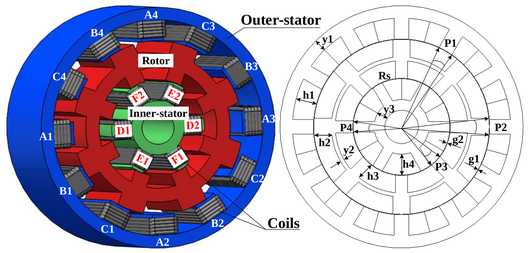

Fig. 1 Sketch structure and geometric parameters of DS-SRM.

Table I Final geometry dimensions of DS-SRM

Name	Parameters	Initial Dimensions
Outer diameter of outer stator	D_{so1}	290 mm
Inner diameter of outer stator	D_{so2}	210 mm
Outer diameter of inner stator	D_{si1}	115.2mm
Diameter of shaft	D_i	40mm
Core length	l_a	170mm
First air gap width	g1	0.4mm
Second air gap width	g2	0.4mm
Outer stator yoke thickness	y1	18 mm
Rotor yoke thickness	y2	4.6 mm
Inner stator yoke thickness	y3	15mm
Outer stator pole-arc coefficient	p1	0.325
Rotor outer teeth pole-arc coefficient	p2	0.305
Rotor inner teeth pole-arc coefficient	p3	0.255
Inner stator Pole-arc coefficient	p4	0.319
Outer stator slot depth	h1	22 mm
Outer rotor teeth depth	h2	21mm
Inner rotor teeth depth	h3	21mm
Inner stator slot depth	h4	22.6 mm

Sensitivity Analyses (1)

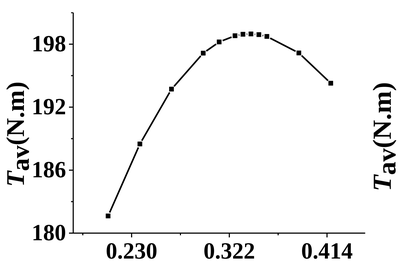

Fig. 2 Different inner-stator pole-arc coefficient

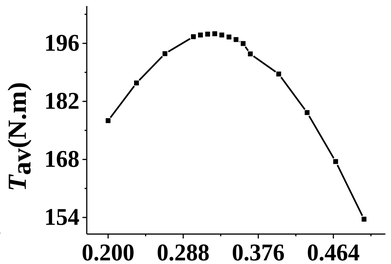

Fig. 3 Different outer-stator pole-arc coefficient

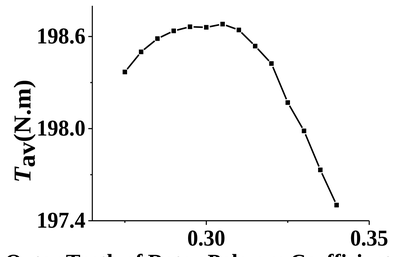

Fig. 4 Different pole arc coefficient of outer teeth of rotor

Sensitivity Analyses (2)

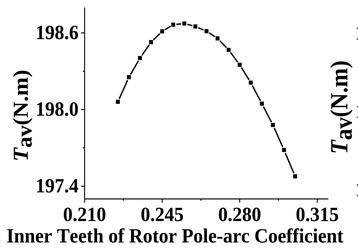

Fig. 5 Different pole arc coefficient of inner teeth of rotor

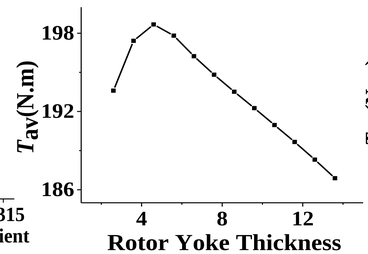

Fig. 6 Different rotor yoke thickness

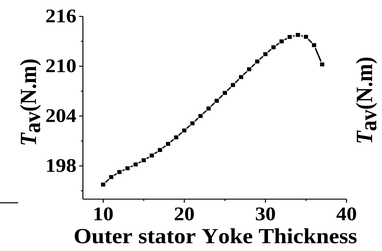

Fig. 7 Different outer-stator yoke thickness

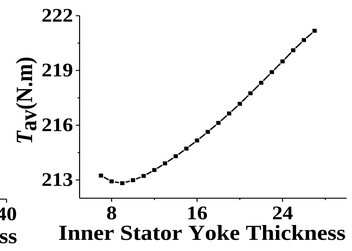

Fig. 8 Different inner-stator yoke thickness

Different Polarity Distribution

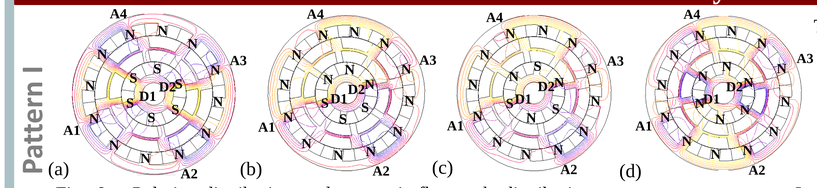

Fig. 9. Polarity distribution and magnetic-flux path distribution on outer-stator pattern I. (a)SSSSSS (b)SSSNNN (c)SNSNSN (d)NNNNNN

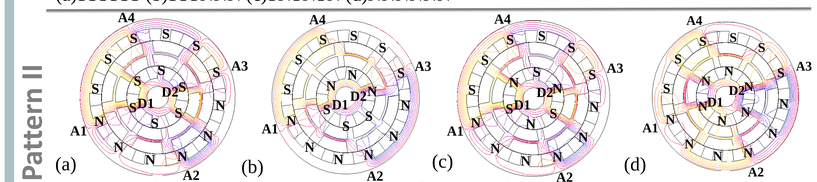

Fig. 10. Polarity distribution and magnetic-flux path distribution on outer-stator pattern II. (a)SSSSSS (b)SSSNNN (c)SNSNSN (d)NNNNNN

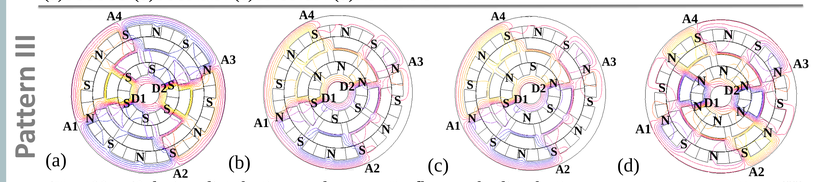

Fig. 11. Polarity distribution and magnetic-flux path distribution on outer-stator pattern III. (a)SSSSSS (b)SSSNNN (c)SNSNSN (d)NNNNNN

Table II Calculated Average Torque on Outer-Stator in Different Patterns

Polarity distribution of outer-stator	Polarity distribution of inner-rotor	T_{1av} (N.m)
NSNSNSNSNSNS	SSSSSS	70.10N.m
	SSSNNN	114.10N.m
	SNSNSN	118.32N.m
	NNNNNN	70.78N.m
NNNNNNSSSSSS	SSSSSS	131.60N.m
	SSSNNN	193.72N.m
	SNSNSN	166.74N.m
	NNNNNN	131.60N.m
SSSSSSSSSSSS	SSSSSS	153.21N.m
	SSSNNN	196.56N.m
	SNSNSN	201.61N.m
	NNNNNN	126.50N.m

Conclusions

Windings layouts of this machine have been studied. It shows that the average torque of rotor with NSNSNSNSNSNS polarity distribution of outer-stator and SNSNSN polarity distribution of inner-stator is the largest which is 201.61N.m. The transient phase current of six phases and transient electromagnetic torque curves are presented. They verify the good performance of the machine.

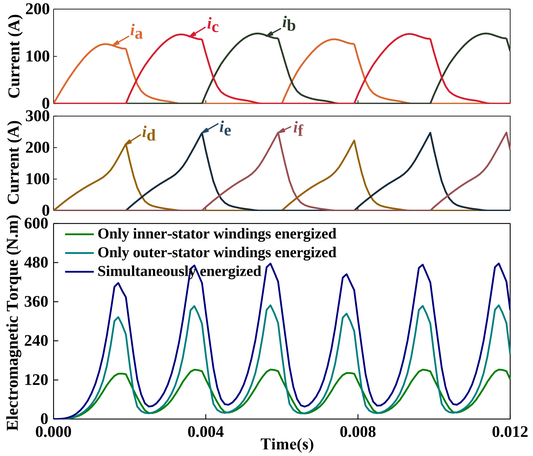

Fig. 12 Transient simulation results